3D pore system reconstruction using nano-scale 2D SEM images and pore size distribution analysis for intermediate rank coal matrix

Alexandra Roslin[a] , Dubravka Pokrajac[a] , Kejian Wu[a], Yingfang Zhou[a*]

[a] School of Engineering, University of Aberdeen, Aberdeen, AB243UE, United Kingdom

[*] Cressponding author through email Yingfang.zhou@abdn.ac.uk

Abstract

This paper comprises the analysis of scanning electron microscopy (SEM) images, nuclear magnetic resonance (NMR) and mercury injection capillary pressure (MICP) data to quantify the pore distribution in coal matrix. We first generate the 3D pore system in the coal matrix based on the statistics of pore distribution obtained from 2D SEM images, and then extract the pore network using the maximal ball method. The influence of the reconstructed cube size and the 2D image resolution on the accuracy of the reconstructed 3D coal sample was analysed when generate the 3D digital coal smaple. It was observed that the highest resolution which was achieved for the studied samples (6nm) resulted in the underestimation of porosity of the studied sample, and it is recommended for future to create several models with different resolution to find the most representative model, instead of apriori using the highest possible resolution. The extracted pore network was then used to analyse pore size distribution and perform capillary pressure simulation using pore network modeling. A comparison of the pore network analysis with NMR and measured MICP data demonstrated that the pore network extraction method simplified the results of distribution and underestimated the size of elongated pores and microfractures. The simulated and laboratory measured MICP shows significant difference partically bucease the network extraction method was not suitable for the studied samples and this could be overcomed by our future study of model MICP using direct simulation method in the reconstructed 3D model.

Key words: Nano-scale, SEM; Pore Size Distributation; Coal Matrix

Introduction

Coal is often described as a dual porosity system where fractures are responsible for the main contribution to the fluid flow while the contribution of coal matrix is often small if any [1]. Previous researchers (e.g. [2]) modelled gas flow in pores in two phases: absorbed gas in coal matrix diffuses to the coal cleats and then viscous flow in cleat network becomes dominant [3]. Pores which are in high abundance in coal matrix can be found: (i) within the macerals and (ii) between macerals or macerals and mineral matter (e.g. [4]). Coal matrix pores can be classified based on the size [5]: (i) micropores are less than 2 nm in diameter; (ii) mesopores are in a range 2-50 nm in diameter and (iii) macropores are greater than 50 nm in diameter. Due to such a small diameter, most of coal

pores cannot be resolved using micro-CT scan images. However, in addition to micro-CT scanning there are other methods to produce very fine scale images of rocks [6]. One of those methods is SEM (scanning electron microscopy) which allows to resolve pores of the size up to nano-meter [7]. A scanning electron microscope scans a focused electron beam over a surface to create a 2D image. The electrons in the beam interact with the sample, producing various signals that can be used to obtain information about the surface topography and composition.

SEM analysis is widely used to determine pore distribution and pore size due to the fact that SEM images are straight forward to interpret compared to NMR (Nuclear Magnetic Resonance) data [8], and can determine pores regardless of their connectivity as opposed to mercury porosimetry [9] and nitrogen absorption [10]. SEM is commonly used 2D scale for pore distribution and morphology analysis (e.g. [3]) but it can also be used for 3D reconstruction using statistical methods. Blunt et al. mentioned that these could be methods that obtain structural patterns or object-based methods which model the packing of grains and diagenesis [6]. For example, the model of Bakke and Oren incorporates grain size distribution and other petrographical data obtained from 2D thin sections in order to reconstruct particle sedimentation process [11]. Object-based methods are extensively used for sandstone reconstruction[12], but they involve intensive computing.

Another approach to 3D reconstruction - extraction of typical patterns - might be more applicable for coal samples due to the difficulty of coal genesis modelling. One of the approaches to reconstruct typical patterns is to ignore the detailed structure of pore space and present porous medium as pore network where large pores are connected through smaller pores (pore bodies and pore throats, respectively) [13-15]. These networks can be used to define pore/throat distribution in order to reproduce multi-phase flow behaviour. Although network models explained some experimental phenomena in multi-phase systems [16-17], while only limited success in prediction of flow properties in real porous media. Wu et al. noted that direct and explicit relationship between pore space images and the reconstruction of suitable network is yet to be found [18].

Multiple point statistics method requires densily and regularly sampled training images which represent the real structure of the samples [19]. The method is applied in two steps: 1) extraction of statistics from training images, and 2) pattern reconstruction [20]. It has demonstrated that this method is quite robust for reconstruction of homogenious samples but might require more information for anisotropic medium.

For the purpose of the research described in this paper, we adopted the Markov chain [18] to reconstruct the 3D nano-scale pore space from 2D SEM images. Generally, this method is based on the idea of using a small amount of local features based on available 2D or 3D images to predict

global conditions[21]. This approach takes into account the relationship between a number of near neighbours to generalise the features of porous medium. This method was previously successfully implemented to reconstruct both homogenious and heterogenious samples and also allowed to quantitatively analyse the reconstructed porous medium. However, so far it has not been used for coal samples.

Sample and coal analysis

Samples of intermediate rank coal from Southern Qinshui coal bed methane basin (China) were obtained and examined using SEM technology. The main characteristics of the our analysed coal sample acquired from coal proximate analysis are listed in Table 1.

Table 1. Coal sample characteristics.

Sample ID	Sample (%)		Organic matter (%)			Vitrinite Reflectance$^{o}_{ran}$ (%)
	Organic matter	Mineral matter	Vitrinite	Inertinite	Liptinite	
PL3#-2	79.87	20.13	77.52	22.48	0.00	1.68

As can be seen, the coal sample contains quite a significant amount of mineral matter which is associated mostly with cleats as it was demonstrated by micro-CT imaging [22-23]. The prevailing organic matter is vitrinite, but inertinite is also presented in considerable amount.

The sample which was chosen for the study was divided into two pieces (see Figure 1A): the upper part of the sample was used to perform NMR (nuclear magnetic resonance) and later MICP (mercury injection capillary pressure). The upper part of the sample was also divided into two pieces, cut, polished in three directions (using a rubber surface to avoid fractures) perpendicular to each other and carbon-coated (Figure 1B). Preparation of three surfaces was required to obtain SEM data in three directions for better representation of pore space. The lower part of the sample was also used for NMR and MICP laboratory experiments but not for SEM analysis.

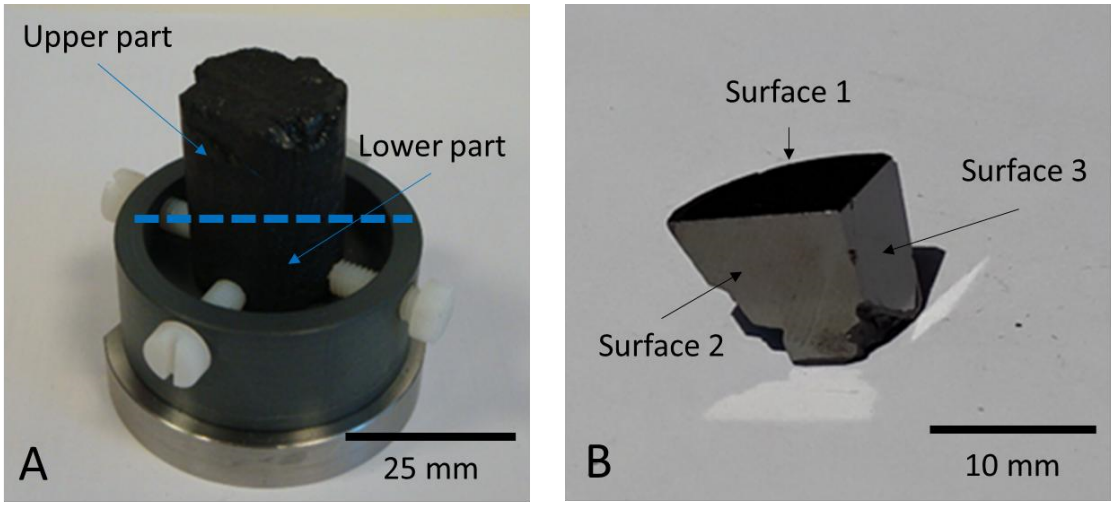

Figure 1. Coal core sample used for the study: A) the original sample in the sample holder which was used for micro-CT analysis, B) the upper part of the original sample polished and carbon-coated for SEM analysis.

Methodology

First of all, the samples were scanned using SEM microscopy (ZEISS Gemini EVO MA10 SEM) to obtain the cross-section images of the nano-size pores within the coal samples under high vacuum condition (magnification range of x20 – x50,000). A beam of focused electrons is emitted from lanthanum hexaboride cathode, rather than classical tungsten hairpin filament. This assures an enhanced image resolution at equivalent probe currents (signal-to-noise). SEM analysis was done in the following manner: scanning of each surface started with magnification x20 to estimate the heterogeneity of the sample and to find representative volume, then the scanning was performed at higher resolution (x1,000 – x5,000) to estimate the details. Later, the smaller features were analysed using magnification x50,000. After analysis of all three surfaces of coal sample, it was found that the samples are quite homogeneous and 8 SEM images were chosen for the purpose of reconstruction. Those 8 images were representative for the studied sample, had the best quality and different resolution that required to reconstruct the 3D samples. Segmentation of SEM images was performed by automatic threshold which is based on Otsu method [24] and after the segmentation procedure the images were binarized. For the purpose of the current research, the images where used to reconstruct a cube which contained 400^3 voxels. The amount of pixels (and voxels for 3D volume) is determined by the homogeneity of the material – previous study has shown that the reconstruction of a homogeneous sandstone might require minimum 100^3 voxels while heterogeneous material might need at least 200^3 voxels [18].

The next stage of reconstruction was the application of stochastic modelling algorithm which is based on Markov chain method [18]. It is an iterative algorithm which is implemented in two phases: 1) the state of each pixel (matrix or pore) is determined from the knowledge about the state of the neighbouring pixels (four pixels in our case) and using the associated four-neighbourhood conditional probability; 2) the state of the next pixel is determined from the knowledge of the previously determined pixel and other neighbouring pixels using the associated five-neighbourhood conditional probability. The conditional probabilities are determined from the original image. The neighbourhood then moved further to the right and then down in a way earlier described [18]. The process repeats until the whole volume is reconstructed (Figure 2).

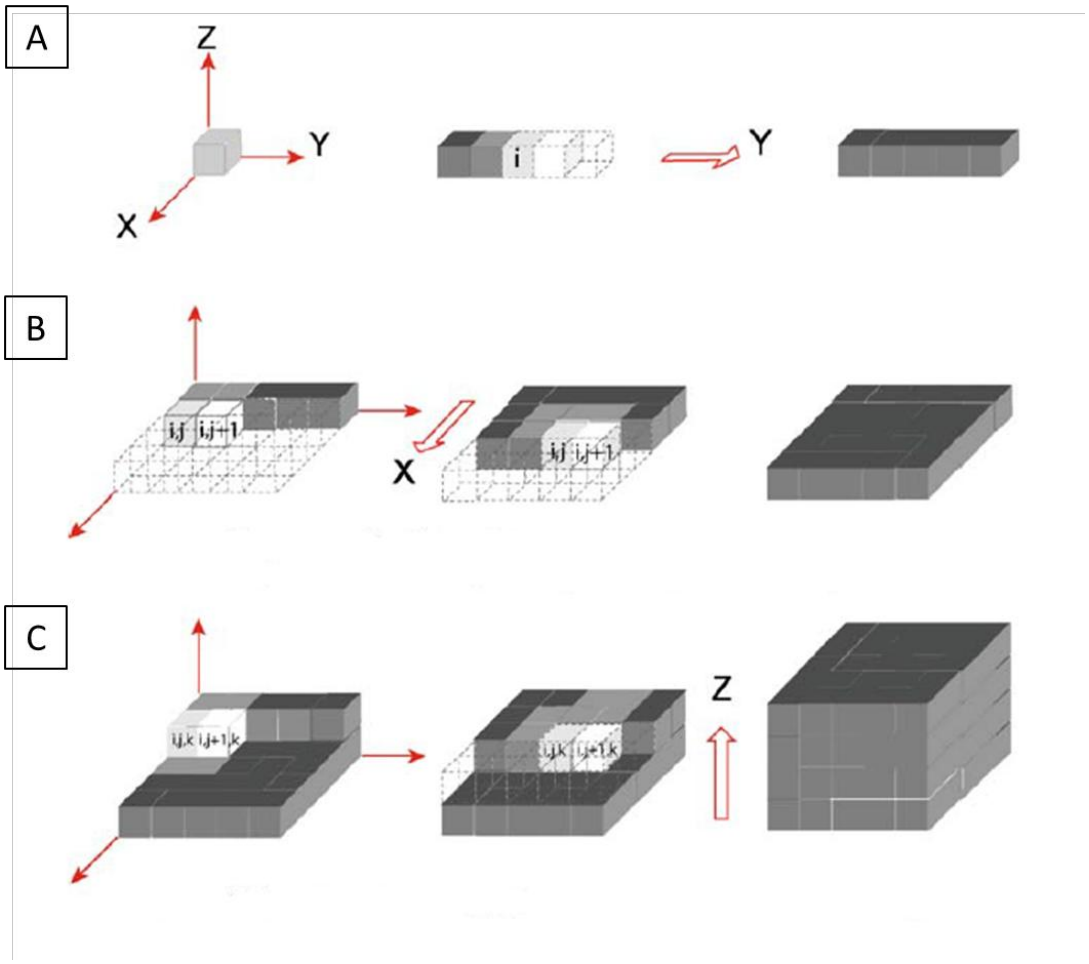

Figure 2. 3D chain construction illustration chart (Adopted from [18]). A) first row of the chain in 1D, 3-neighbourhood; B) first layer of the chain in 2D, 3- and 4-neighbourhood on edge, 5- for (I,j) and 6-neighbourhood for (I, j+1) within the frame; C) upper layer of the chain in 3D, 10-neighbourhood on edge and 15-neighbour within the interior structure.

The accuracy of the reconstruction was controlled by comparison to nuclear magnetic resonance (NMR) data as will be explained later. NMR is a physical phenomenon in which nuclei in a strong

static magnetic field are perturbed by a weak oscillating magnetic field (in the near field and therefore not involving electromagnetic waves [25] and a magnetic field creates a dipole moment in hydrogen in fluid components. The amplitude of the dipole moment is proportional to the number of hydrogen atoms in the fluid and it can be considered as the pore volume filled with fluid [8]. The dipole moment temporal variation can be converted into longitudinal (T1) and transverse (T2) relaxation time distributions. Generally, the T2 distribution reflects the pore size distribution and the smallest pores have the shortest T2 while the largest pores have the longest T2.

Mercury injection capillary pressure (MICP) method is typically used to establish the relationship between capillary pressure and the porous structure of the sample [26]. In MICP the pores of the sample are emptied and then imbued with mercury with increasing pressure until the injected pressure reaches 200 MPa. The volume of mercury at each given pressure is recorded and the resulting capillary pressure curves can be compared to the modelled pressure curves.

Results

As it was mentioned above, 8 SEM images from three orthogonal surfaces were chosen for the purpose of the current research (Table 2), and they were analysed, segmented and binarized. Images F and B were taken from surface 1 (X-direction), A, C and E – from surface 2 (Y-direction), D, G and H – from surface 3 (Z-direction) (Figure 3). Then, 5 different sets of images were combined based on the image resolution (Table 3) since generation of 3D pore geometry requires that all input images have similar resolution.

Table 2. SEM image characteristics.

Image	Resolution (nm)	Porosity (%)
A	28	1.4
B	6	0.3
C	33	2.0
D	26	1.0
E	6	1.3
F	18	2.3
G	33	1.6
H	6	2.9

Table 3. Sets formed from SEM images.

Set	X image	Y image	Z image	Average porosity from images (%)	Porosity from reconstructed model (%)
1	F	A	D	1.57	1.60
2	F	A	G	1.76	1.67
3	F	C	D	1.76	1.78
4	F	C	G	1.96	1.78
5	B	E	H	1.48	1.26

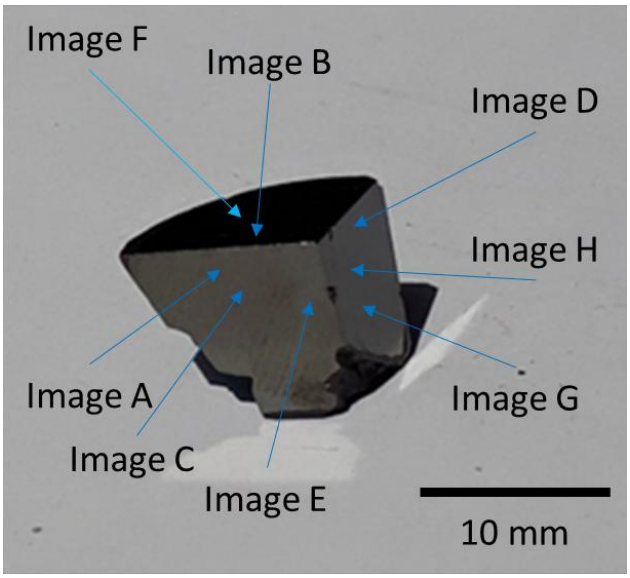

Figure 3. The studied sample and the locations of the images used for the reconstruction.

The next step of 3D image reconstruction was to run the algorithm [18] which requires at least one image in each orthogonal direction as it is generally based on the analysis of the image statistics to build a 3D cube. As it was mentioned before, the size of the cube depends on the heterogeneity of the material and it is recommended that the cube has at least 200^3 voxels. Due to the fact that coal can be quite heterogeneous 400^3 voxels cube was built for the purpose of current research. The algorithm was run for each set of images and the outcomes were validated by comparison to available porosity and pore size distribution data. Firstly, the porosity of the resulting model was compared to the average porosity obtained from image analysis (Table 3). Secondly, the porosity of reconstructed models was assessed by a comparison to the NMR results which gave a value of 1.63%. As it can be observed, NMR porosities are congruent with the average porosity from images and from the reconstructed models (Table 3). Figure 4 illustrates reconstructed 3D cubes for all sets

and demonstrates that pores are sparsely distributed which is correlated to what was observed on SEM images. Figure 5 shows the distribution of coal matrix pores in 3D.

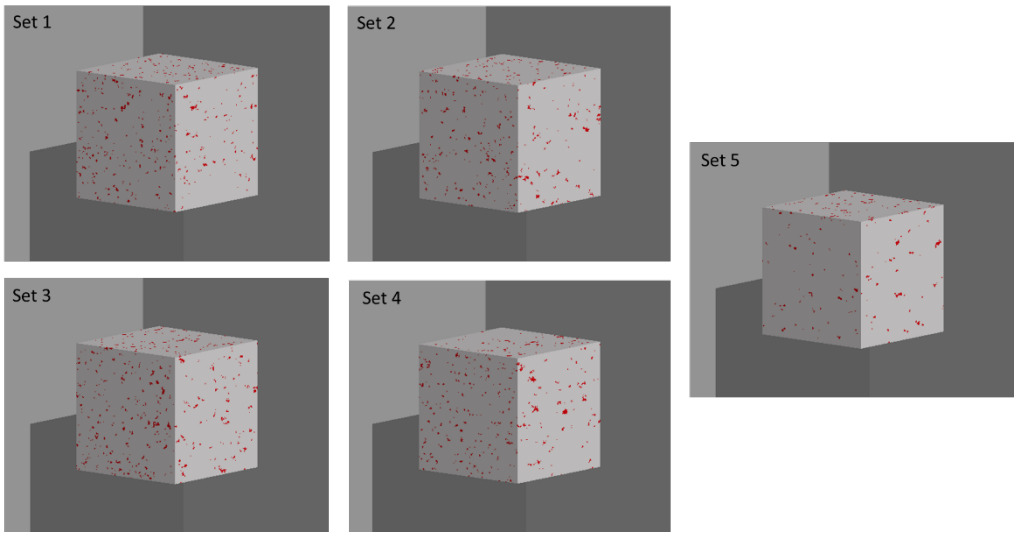

Figure 4. Reconstructed 3D cubes for five different sets. Pores are shown in red colour.

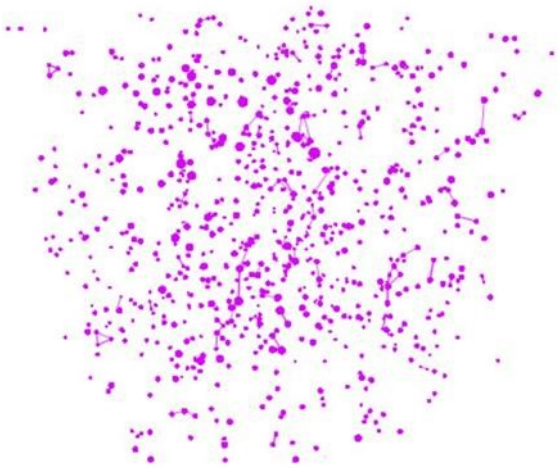

Figure 5. Extracted pore network for the reconstructed 3D model.

After the comparison of porosity, the pore size distribution of the reconstructed 3D model was analysed. First of all, network extraction was performed using the code established by Dong and Blunt [27] and updated recently by the same group at Imperical College [28] which is principally based on the maximal ball concept [29]. The code provided pore and throat size distribution statistics which were compared to MICP and NMR data. Analysis of pore size distribution of reconstructed model demonstrated that the reconstructed coal matrix contains mostly pores in a range of 5 – 10 nm and in the range of 32 – 70 nm (Figure 6). In addition to micropores, some amount of microfractures were observed on SEM images and their width was determined visually to be in the range of 1-10 micron (Figure 7). Maximal ball approach which was previously used for the pore network extraction method was not applied to determine the microfracture width as it works

accurately for isometric pores but not for fractures. In turn, analysis of NMR data demonstrated that pore distribution is characterised by two picks: one of them is about 1-2 nm and another one is about 1 micron (Figure 8). The maximum resolution which was obtained for SEM was about 5.5 nm which means that it was not possible to recognise pores in the range 1-2 nm. The second NMR peak may be due to the observed microfractures.

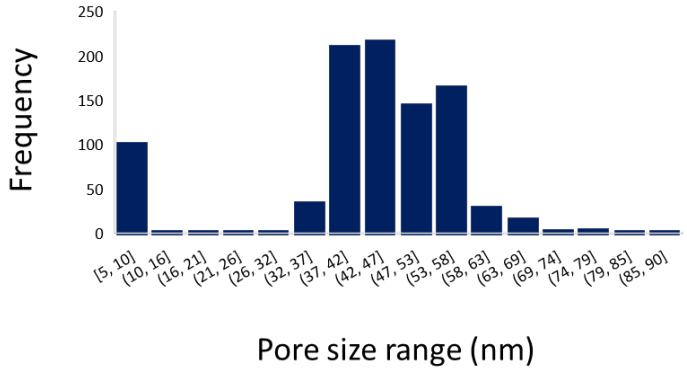

Figure 6. Pore size distribution from reconstructed 3D models.

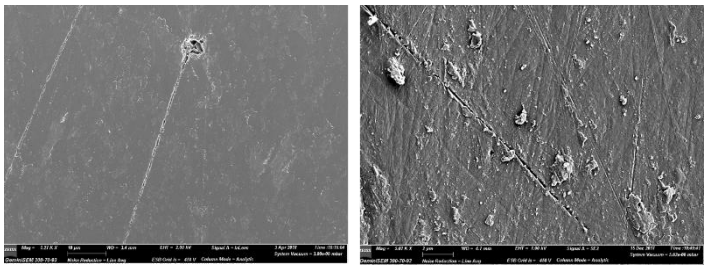

Figure 7. Microfractures on SEM images.

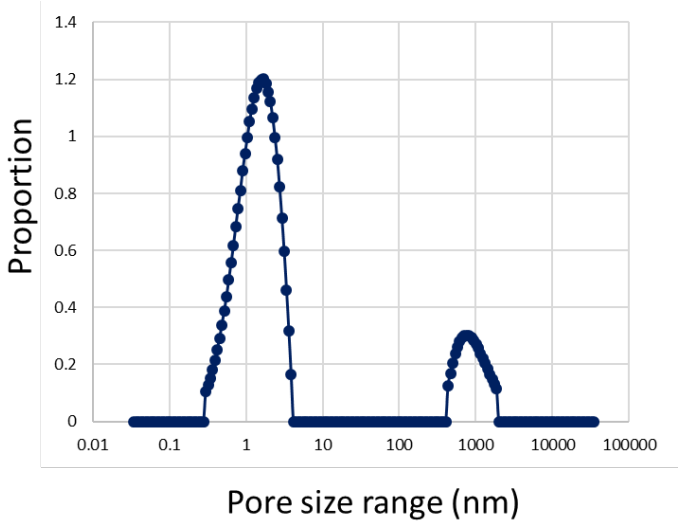

Figure 8. Pore size distribution obtained from NMR data.

Another comparison was made to MICP data (Table 4 and Figure 9). What was observed is in a good comparison with NMR pore distribution: the main portion of pores (58.36%) are smaller than 25nm but there is also a significant amount of pores in the range of 25 – 100nm (8.93%). Pores in a range about 1 micron (0.5 – 2.5 microns) comprise about 9%. The MICP pore size distribution therefore confirmed the conclusion that pore network extraction method which we utilised underestimated the size of matrix pores. However, for further control of the results and the conclusions the extracted pore network was exploited for pressure curves simulation and comparison to MICP pressure curves (Figure 10). A network simulator developed by Ahmed Boujelben at Heriot-Watt University was used for the purpose of pressure curves simulation (https://github.com/ahboujelben/numSCAL_basic).

Table 4. Pore size distribution obtained from MICP data.

Number	R，μm	Frequency，%
1	0.00-0.025	58.36
2	0.025-0.10	8.93
3	0.10-0.25	2
4	0.25-0.50	2.05
5	0.50-1.00	3.17
6	1.00-2.50	5.82
7	2.50-6.50	5.38
8	6.50-16.00	4.67
9	16.00-50.00	9.61

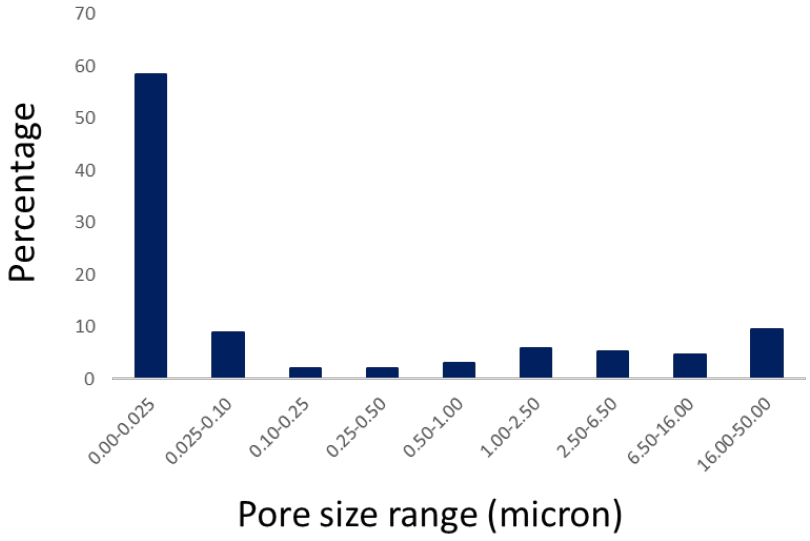

Figure 9. Pore size distribution obtained from MICP data.

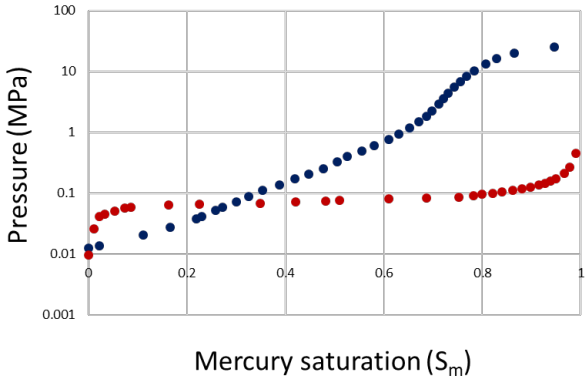

Figure 10. Capillary pressure curves: blue – obtained from MICP analysis, red – calculated based network extracted from 3D reconstructed model.

Figure 10 demonstrates significant discrepancy between simulated and MICP pressure curves, as expected. It is planned for the future to perform simulation of fluid flow directly on 3D reconstructed model using level-set method which is supposed to produce the results that closer to the laboratory data.

Discussion

Probably the most promising and popular method to analyse the internal structure of the rock samples is micro-computed tomography, which allows obtaining the 3D structure of rock specimens quickly and non-destructively. However, the main disadvantage of that method is the limited resolution. Although modern X-ray scanners may achieve resolution of up to 1 micron, this resolution is not enough to resolve the pores of the coal matrix. In that case, scanning electron

218 microscopy can be used to reveal the detailed structure of the coal matrix pore network. The main
219 issue of SEM application is an impossibility to obtain the 3D internal structure of the studied objects.
220 At present, the 3D SEM models can be obtained only by reconstruction from 2D SEM images. There
221 are different approaches to reconstruct 3D models from 2D images by the implementation of
222 statistical methods. For the current research, the algorithm which is based on the Markov chain
223 method was chosen. The choice of the algorithm is explained by the fact that this algorithm was
224 successfully utilised for heterogeneous samples. However, to the best of the authors' knowledge,
225 statistical reconstruction of the 3D models from 2D SEM images has never been applied to coal
226 samples. Current research tried not only to reconstruct the 3D models but also to estimate the
227 suitable volume of reconstruction and the effect of the resolution of the final results. The author of
228 the algorithm claimed that for the heterogeneous samples, the reconstructed cube should have at
229 least 200^3 voxels. However, in the current research, it was found that the cubes of 200^3 voxels had
230 the porosity about 1%, the cubes of 300^3 voxels had the porosity about 1.2%, while the cubes of 400^3
231 voxels had the porosity about 1.6-1.7% which is better correlated to the average porosity obtained
232 from NMR (1.67%). Increase of cube size to 500^3 and 600^3 voxels did not change the porosity of the
233 models, so for the future research in coal, the volume 400^3 voxels is probably an optimal size for
234 accurate resolution.

235 Another uncertainty of 3D model reconstruction was the resolution of images required for the
236 reconstruction. The analysis demonstrated that very high resolution (about 6nm) produced the
237 model which underestimated the sample porosity. Models built on the images with lower resolution
238 (18-33nm) gave porosity closer to the NMR average porosity (Table 3). For the future, it might be
239 recommended to build the models of different resolution and compare the results instead of relying
240 on the images of the highest resolution.

241 The reconstructed models were further used to assess pore size distribution. The maximal ball
242 method was used to extract pore network and estimate pore diameter, and the obtained results
243 were compared to NMR and MICP data collected for the studied sample. The pore size distribution
244 which was obtained from the analysis of the extracted pore network showed that the majority of
245 pores are in the range of about 30-70nm, which generally correspond to the MICP pore size
246 distribution (Table 4). However, the smallest and the largest pores (macropores and microfractures)
247 disappeared from the reconstructed model pore size distribution. It could be explained because the
248 smallest pores were beyond the resolution of the SEM images, while the largest pores and
249 microfractures were not correctly recognised by the maximal ball method. As a result, the simulation
250 performed on extracted from the reconstructed model pore network demonstrated a considerable
251 discrepancy with MICP data (Figure 10).

Figure 10 shows a comparison of MICP pressure curves and the simulated pressure curve. Since a drainage process was simulated (the non-wetting phase displaced the wetting phase), the largest pores were occupied by mercury at lower pressure. Then pressure gradually increased, and the smaller pores were filled by mercury as it was demonstrated by the MICP pressure curve. In turn, the simulated pressure curve quickly jumped from zero to some plateau area and started gradually increasing only at the very end where it suddenly stopped. This behaviour was explained by the fact that the network extraction method could extract only some middle range of pores. It is planned for the future to perform simulation of fluid flow directly on the 3D reconstructed model using the level-set method, which is supposed to produce the results that are closer to the laboratory data.

Conclusion

The research described in the paper focuses on the reconstruction of 3D models from 2D SEM images and analysis of pore size distribution obtained from the reconstructed models. Images which were used for reconstruction were taken from three orthogonal surfaces of the intermediate-rank coal sample, and the algorithm which is based on the Markov chain method was utilised to reconstruct the 3D models. In the course of the research, 5 different models of the different resolution were created, and it was found that for the studied sample, the resolution of the images does not influence on the results of reconstruction. Thus, the average porosities of the model with 6nm resolution and the model with 30nm resolution are similar. Still, there is a tendency to underestimate the porosity of the sample, if the images of high resolution (6nm) are used. The reconstructed models were utilised to analyse the pore size distribution of the coal matrix, and the maximal ball method was used to extract pore network. It was found that the maximal ball method significantly underestimates pore size as compared to NMR and MICP pore size distribution. The conclusion about the underestimation of pore sizes is indirectly confirmed by the results of drainage process simulation. Simulated pressure curve demonstrated huge discrepancy with MICP pressure curve, which was explained by the fact that the simulated curve reflects the only occupation of the biggest pores whose size was underestimated. It is planned in the future to repeat simulation of fluid flow in coal matrix using the level-set method, which does not require to extract pore network.

Acknowledgment

This paper utilised opportunistic coal samples and characterisation data as a part of a study into multiphase flow in coal for Southern Qinshui coal basin. The measurement of this work was supported by the Royal Society and Royal Society Edinburgh through the International Cost Share Project, and Alexandra would like to thank Ministry of Education of Russia to support her PhD work at University of Aberdeen. The University of Aberdeen School of Engineering and School of

Geosciences are thanked for their support. The authors also thank John Still from The University of Aberdeen School of Geosciences for his support regarding SEM data analysis.

Reference

1. Ramandi H.L., Mostaghimi P., Armstrong R.T., Pinczewski W.V., 2016. Porosity and permeability characterization of coal: A micro-computed tomography study. International Journal of Coal Geology, 154-155, 57-68.
2. Karachan, C.O., Okandan, E., 2001. Adsorption and gas transport in coal microstructure: investigation and evaluation by quantitative X-ray CT imaging. Fuel, 80, 509-520.
3. Giffin S., Littke R., Klaver J., Urai J.L., 2013. Application of BIB-SEM technology to characterise macropore morphology in coal. International Journal of Coal Geology, 114, 85-95.
4. Gamson P.D., Beamish B.B., Johnson D.P., 1993. Coal microstructure and micropermeability and their effects on natural gas recovery. Fuel 72, 87 – 99.
5. Rouquerol J., Avnir D., Fairbridge C.W., Everett D.H., Haynes J.H., Pernicone N., Ramsay J.D.F., Sing K.S.W., Unger K.K., 1994. Recommendations for characterisation of porous solids. Pure and Applied Chemistry 68, 1739 – 1758.
6. Blunt M.J., Bijeljic B., Dong H., Gharbi O., Iglauer S., Mostaghimi P., Paluszny A., Penland C., 2013. Pore-scale imaging and modelling. Advanced in Water Resources, 51, 197-216.
7. Zhou S., Yan G., Xue H., Guo W., and Li X., 2016, 2D and 3D nanopore characterization of gas shale in Longmaxi formation based on FIB-SEM. Marine and Petroleum Geology 73, 174-180.
8. Yao Y., Liu D., Che Y., Tang D., Tang S., Huang W., 2010, Petrophysical characterization of coals by low-field nuclear magnetic resonance (NMR). Fuel 89, 1371 – 1380.
9. Prinz D., Littke R., 2005. Development of the micro- and ultramicroporous structure of coals with rank as deduced from the accessibility to water. Fuel 84, 1645-1652.
10. Prinz D., Pyckhout-Hintzen W., Littke R., 2004. Development of the meso- and macroporous structure of coals with rank as analysed with small angle neutron scattering and adsorption experiments. Fuel 83, 547-556.
11. Bakke S., Oren P.-E., 1997. 3-D pore-scale modelling of sandstones and flow simulations in the pore networks. SPE Journal 2, 136–149.
12. Oren P.-E., Bakke S., 2002, Process based reconstruction of sandstones and prediction of transport properties. Transport in Porous Media 46 (2–3), 311–343.
13. Blunt M., Zhou D., Fenwick D., 1995. Three-phase flow and gravity drainage in porous media. Transport in Porous Media 20, 77–103.

14. Oren P.-E., Billiotte J., Pinczewski W.V., 1994. Pore-scale network modelling of waterflood residual oil recovery by immiscible gas flooding. Paper SPE 27814, Proceedings of the Ninth SPE/DOE Symposium on Enhanced Oil Recovery, Tulsa, April 17–20.
15. van Dijke M.I.J., Sorbie K.S., 2002. Pore-scale network model for three-phase flow in mixed-wet porous media Physical Review E 66, 046302.
16. McDougall S.R., Sorbie K.S., 1995. The impact of wettability on waterflooding: Porescale simulation, SPE Reservoir Engineering, August, 208–213.
17. van Dijke M.I.J., Sorbie K.S., Sohrabi M., Danesh A., Tehrani D., 2004. Three-phase flow WAG processes in mixed-wet porous media: pore-scale network simulations and comparisons with water-wet micromodel experiments. SPE Journal 9, 57–66.
18. Wu K., Van Dijke M.I.J., Couples G.D., Sorbie K.S., Ma J., 2006. 3D stochastic modelling of heterogeneous porous media – applications to reservoir rocks. Transport Porous Media, 65 (3), 443–67.
19. Okabe H., Blunt M.J., 2004a. Predicting permeability through 3D pore-space images reconstructed using multiple-point statistics, International Symposium of the Society of Core Analysts, Abu-Dhabi, 5-9 October.
20. Okabe H., Blunt M.J., 2004b. Prediction of permeability for porous media reconstructed using multiple-point statistics. Physical Review E 70, 066135.
21. Wu, H., Zhou, Y., Yao, Y. and Liu, D., 2004. Imaged based fractal characterization of micro-pore structure in coal sample, Fuel 239, 53-62.
22. Roslin, A., Pokrajac, D. and Zhou, Y., 2019. Permeability upscaling using cubic law based on the analysis of multi-resolution micro-CT images of intermediate rank coal, Energy & Fuels, 33 (9), 8215-8221.
23. Roslin, A., Pokrajac, D. and Zhou, Y., 2019. Cleat structure analysis and permeability simulation of coal samples based on micro-computed tomography (micro-CT) and scan electron microscopy (SEM) technology, Fuel, 254, 15, 115579.
24. Otsu N., 1979. A Threshold Selection Method from Gray-Level Histograms. IEEE Transactions on Systems, Man, and Cybernetics: Systems 9, 62–66.
25. Hoult D.I., Bhakar B., 1997. NMR signal reception: Virtual photons and coherent spontaneous emission. Magnetic Resonance9 (5), 277 – 297.
26. Purcell W.R., 1949. Capillary Pressures - Their Measurement Using Mercury and the Calculation of Permeability Therefrom. Society of Petroleum Engineers.
27. Dong H., Blunt M.J., 2009. Pore-network extraction from micro-computerized tomography images. Physical Review E 80, 036307.

28. Raeini A.Q., Bijeljic B., Blunt M.J., 2017. Generalized network modeling: Network extraction as a coarse-scale discretization of the void space of porous media. Physical Review E 96, 013312.
29. Silin D., Patzek T., 2006. Pore space morphology analysis using maximal inscribed spheres. Physica A 371, 336–60.